Brodogradnja Volume 76 Number 1 (2025) 76102

journal homepage: www.brodogradnja.fsb.hr

Brodogradnja

An International Journal of Naval Architecture and Ocean Engineering for Research and Development

Enhancing sustainability in LNG carriers through integrated alternative propulsion systems with Flettner rotor assistance

Nader R. Ammar[1,2*], *Ibrahim S. Seddiek*[3]

[1] *Department of Marine Engineering, Faculty of Maritime Studies, King Abdulaziz University, 21589 Jeddah, Saudi Arabia.*
[2] *Department of Naval Architecture and Marine Engineering, Faculty of Engineering, Alexandria University, 21544 Alexandria, Egypt.*
[3] *Department of Marine Engineering Technology, Faculty of Maritime Transport & Technology, Arab Academy for Science, Technology & Maritime Transport, 1029 Alexandria, Egypt.*

ARTICLE INFO

Keywords:
Integrated propulsion systems
Flettner rotors
LNG carrier
Environmental analysis
Economic analysis

ABSTRACT

The maritime industry is actively seeking sustainable solutions to reduce ship emissions and enhance energy efficiency. This study explores the use of alternative fuels and renewable energy sources, focusing on the potential environmental and economic benefits of combining natural gas (NG) fuel with Flettner rotor (FR) technology. The research employs technical, environmental, and economic models to evaluate various scenarios integrating NG fuel with FR in alternative propulsion systems. It investigates three propulsion configurations for LNG vessels: diesel engine (DE-FR), dual fuel diesel engine (DFE-FR), and combined gas and steam turbine engines (COGAS-FR). Results indicate that utilizing six Flettner rotors produces 1.254 MW, resulting in fuel savings of 3.49% to 4.49%, along with notable emission reductions. The COGAS-FR system emerges as the most environmentally friendly option, enhancing energy efficiency by 4.68% based on current ship standards. From an economic perspective, transitioning to the DFE-FR system is identified as an optimal eco-friendly choice, leading to a 9.85% reduction in the levelized energy cost compared to DE-FR. However, it is noteworthy that the COGAS-FR system has the most significant environmental impact, with a cost-effectiveness of $10,954.6 per ton.

1. Introduction and literature review

Ship emissions are a significant contributor to global warming and climate change as they release substantial amounts of greenhouse gases (GHG) into the atmosphere. These emissions, which include carbon dioxide (CO_2), sulfur oxides (SO_x), and nitrogen oxides (NO_x) have adverse effects on the environment and human health [1, 2]. In terms of environmental impact, maritime transportation accounts for almost 3% of global CO_2 emissions [3, 4]. To tackle this pressing issue, the International Maritime Organization (IMO) has implemented emission regulations aimed at reducing the environmental impact of shipping activities. Notably,

* Corresponding author.
E-mail address: nammar@kau.edu.sa

http://dx.doi.org/10.21278/brod76102
Received 13 June 2024; Received in revised form 5 October 2024; Accepted 17 October 2024
Available online 22 October 2024
ISSN 0007-215X; eISSN 1845-5859

the IMO has established regulations for controlling NO_x and SO_x emissions, imposing limits on the amount of these pollutants that ships can emit [5, 6]. Additionally, the IMO has set a target to achieve a 50% reduction in greenhouse gas emissions from global shipping by 2050 compared to the levels recorded in 2008. In response, the IMO has introduced the Energy Efficiency Existing Ship Index (EEXI) and the Carbon Intensity Indicator (CII) to promote energy efficiency and decrease carbon intensity within the shipping industry [7-10].

Renewable energy sources have garnered significant attention as a means to reduce ship emissions and promote sustainable practices in the maritime industry [11, 12]. One innovative solution that has gained traction is the use of the Flettner rotor (FR) as a form of onboard wind propulsion. FR is a vertical cylinder that utilizes the Magnus effect to harness wind energy and generate forward thrust. Fig. 1 shows the principle of the Magnus effect and a rotor sail installed onboard a very large ore carrier (VLOC) named Sea Zhoushan [13]. By harnessing wind power, ships can reduce their reliance on traditional fossil fuel-based propulsion systems and decrease greenhouse gas emissions significantly [14, 15]. Several studies have explored the potential of FR in reducing ship emissions [16-18]. For instance, research works of [19, 20] investigated the design, operation, and parametric studies of wind-assisted ships. Similarly, studies by [21-25] highlighted the experimental and aerodynamic performance investigations of FR for maritime applications. These findings underscore the role of FR as a promising renewable energy solution for mitigating ship emissions and advancing sustainable shipping practices. A study by [26] investigated a novel approach to optimizing FR layout using wake energy, enhancing aerodynamic performance, and increasing lift coefficient. Another study by [27] used Computational Fluid Dynamics to analyze a standalone FR, validating predictions with experimental data. Moreover, [28] examined Flettner Rotors' impact on ship roll motion in beam waves using XFlow CFD, indicating decreased lift power with increased heeling angle. [29] explored combining weather routing and wind propulsion for emission reductions, stressing adaptive strategies' significance. The research revealed that optimal wind routes with longer durations are greatly influenced by uncertain forecasts, potentially reducing FR and weather routing savings. [30] introduced an innovative empirical method for studying wind-assisted cargo ships, emphasizing the method's versatility in research applications. Additionally, [31] proposed a zero-emission hybrid hydrogen-wind-powered propulsion system for a merchant ship, demonstrating feasibility with reduced deadweight and enhanced sustainability.

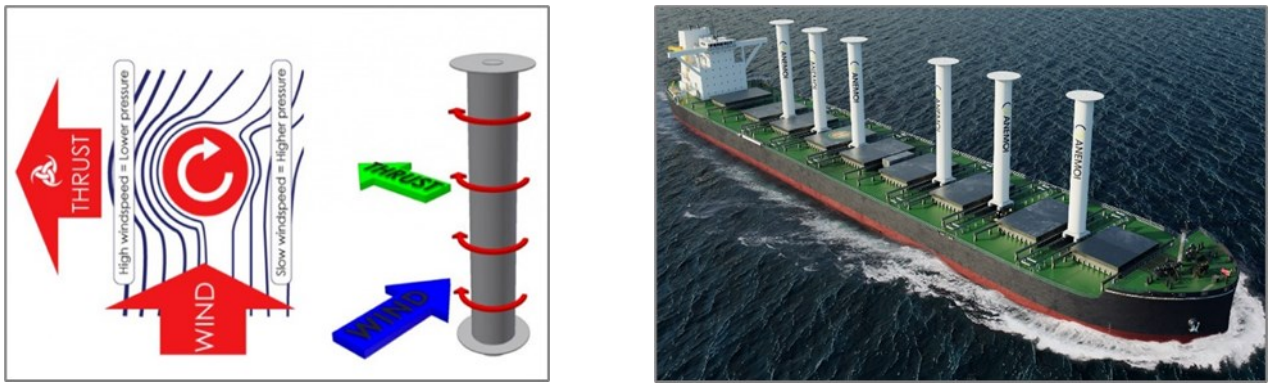

Fig. 1 Magnus effect and FR onboard ships

In addition, the utilization of natural gas (NG) as an alternative fuel in the maritime industry has garnered significant attention as a means to reduce ship emissions and improve environmental sustainability. It has emerged as a promising option due to its lower carbon intensity and reduced emissions compared to conventional marine fuels [32-34]. Natural gas can also be employed in dual fuel and combined gas and steam (COGAS) marine engines as a viable solution for reducing emissions. Dual fuel engines offer the advantage of utilizing both natural gas and liquid fuels, providing flexibility and the potential for substantial emissions reduction. Studies conducted by [35-38] have investigated the performance and emissions characteristics of natural gas/diesel dual-fuel engines, highlighting their potential for achieving lower NO_x and SO_x emissions. Additionally, studies by [39-42] have explored the techno-environmental, design, and economic aspects of COGAS systems for ships, revealing their potential to reduce fuel consumption and emissions. Moreover,

energy, exergy, economic, and environmental analyses of an NG regasification system in floating storage regasification units are investigated [43]. Collectively, these studies contribute to our understanding of the applications of natural gas in marine engines, emphasizing their potential for the reduction of emissions and the promotion of environmental sustainability.

From the previous introduction and literature review, it is evident that the maritime industry is facing cumulative pressure to decrease emissions and improve sustainability to mitigate the environmental impact of shipping. In this context, the exploration of alternative fuels and renewable energy sources has gained significant attention. However, there is a research gap in the integration of alternative natural gas (NG) fuel and renewable FR technology in the context of LNG carriers. While studies have examined the individual benefits of NG fuel and FR technology, there is limited research on the combined utilization of these technologies in LNG carriers. Therefore, the current research paper uniquely investigates merging NG fuel and FR technology in LNG carriers to assess environmental and economic advantages. Through a detailed case study, this research offers crucial insights into the viability and efficacy of this integrated strategy for sustainable maritime transport.

2. Methodologies

Fig. 2 shows the methodology flow chart for the present paper. It visually outlines the research approach and steps involved in evaluating the integration of FR in ship propulsion. The flow chart begins by defining the research objective, focusing on evaluating the impact of FR technology on ship propulsion. It then develops technical, environmental, and economic models critical for assessing FR-assisted propulsion feasibility. Scenario analysis follows, evaluating various FR-assisted configurations, considering energy generation, fuel savings, emission reductions, and efficiency improvements. Integration of FR and an environmental impact analysis are also included. Subsequently, the economic evaluation compares costs and benefits, emphasizing the cost-effectiveness of the system. The chart concludes with research findings, highlighting the most efficient and cost-effective propulsion system for ships.

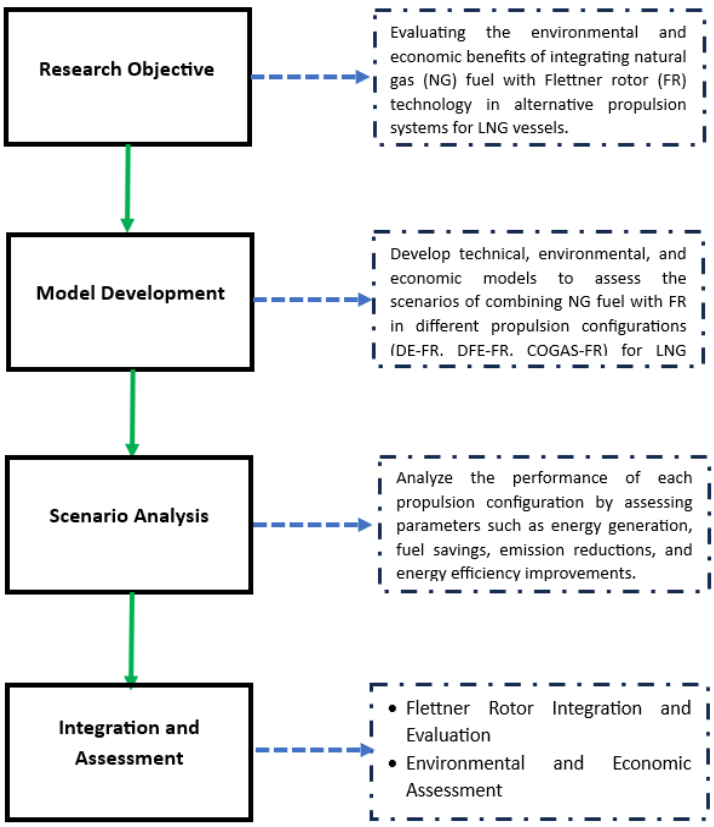

Fig. 2 Methodology flow chart for the present paper

The remainder of this section focuses on the development of technical, environmental, and economic equations to model the performance and assess the benefits of FR. By developing models, the power output, energy savings, and environmental benefits can be evaluated. The goal is to assess the viability and potential of FR technology as a sustainable solution for the shipping industry. Three different propulsion engines are included in the current paper: the diesel engine (DE), dual fuel diesel engine (DFE), and combined gas and steam turbine engines (COGAS). The subsequent section focuses on the economic characteristics of the DFE as well as COGAS propulsion options. Additionally, the section concludes with an assessment of the life cycle cost-effectiveness for the proposed propulsion engines.

2.1 Techno-environmental modelling

FR onboard ships harness the power of the wind to generate thrust and improve energy efficiency. To accurately model their performance, it is essential to consider the true and apparent wind speeds practiced by the rotors. The true wind speed (V_{tw}) represents the actual speed and direction of the wind in relation to the Earth's surface. The apparent wind speed (V_{aw}) is the wind speed observed by an observer on the moving ship. It takes into account the ship's speed (V_s) and the relative angle between this speed and the true wind speed (θ_r). The calculation for V_{aw} can be expressed as shown in Eq. 1 [18, 44]:

$$V_{aw} = \sqrt{V_{tw}^2 + V_s^2 - 2V_{tw}V_s cos\theta_r} \tag{1}$$

Two forces are produced by the FR onboard the ship: the drag force (D), which operates in alignment with the local wind direction, and the lift force (L), which acts perpendicular to the local apparent wind direction. The lift and drag forces generated by FR can be calculated using Eqs. 2 and 3 [45, 46]:

$$L = 0.5\rho_a A_r V_{aw}^2 C_L \tag{2}$$

$$D = 0.5\rho_a A_r V_{aw}^2 C_D \tag{3}$$

where ρ_a represents the air density, A_r denotes the effective rotor area, V_a represents the apparent wind speed, and C_D and C_L symbolize the drag and lift coefficients, respectively. The lift and drag coefficients can be determined based on the spin ratio, as explained in previous studies [44, 47].

Each FR produces a power (P_{prod}) and consumes another one (P_{cons}) to rotate it around its axis as expressed in Eqs. 4 and 5:

$$P_{cons} = 0.5\rho_a A_r V_{aw}^3 C_p \tag{4}$$

$$P_{prod} = F_x \,.\, V_s \tag{5}$$

where C_p is the power coefficient. It can be determined based on the spin ratio, as described in previous studies [44, 47]. F_x represents the resultant force generated by the FR in the direction of the ship. By analyzing a matrix that includes the apparent wind angle (β), along with the lift and drag forces, we can calculate the resultant force acting in the direction of the ship's movement (F_x) and perpendicular to it (F_y), as illustrated in Eq. 6:

$$\begin{bmatrix} F_x \\ F_y \end{bmatrix} = \begin{bmatrix} cos\beta & sin\beta \\ -sin\beta & cos\beta \end{bmatrix} \begin{bmatrix} -D \\ L \end{bmatrix} \tag{6}$$

The produced propulsion power from FR in ship direction ($P_{prop,FR}$) in kW can be estimated by considering the ship's propulsive efficiency (η_s), as illustrated in Eq. 7 [48]:

$$P_{prop,FR} = \left(P_{prod} - P_{cons}\right).\eta_s \tag{7}$$

The annual fuel saving after installing number of FR (n) onboard a ship (AFS_{FR}) can be calculated using Eq. 8:

$$AFS_{FR} = \sum_{i=1}^{i=n} P_{prop,FR} \,.\, SFC_{ME} \cdot T \tag{8}$$

where, SFC_{ME} is the specific fuel consumption for DE, DFE, and COGAS engines, in kg/kWh and T is the annual operating time for the FR.

On the other hand, the annual reduction in exhaust gas emissions after implementing FR (ARE_{FR}) onboard a ship can be estimated using Eq. 9 [49, 50]:

$$ARE_{FR} = \sum_{i=1}^{i=n} P_{prop,FR} \,.\, E_f . T \tag{9}$$

where, E_f represents the emission factors for the DE, DFE, and COGAS engines in kg/kWh. SO_x, NO_x, HC, PM CO, and CO_2 emission factors can be found in [51-54].

The assessment of CO_2 emissions from ships is conducted through the utilization of energy efficiency indexes. There are two standards for the *EEXI*: the reference value ($EEDI_{ref}$) and the attained value ($EEDI_{attained}$). The attained *EEXI* should be equal to or lower than the reference EEXI rate. The reference value, expressed in gCO_2/ton.NM, can be calculated for LNG carriers as shown in Eq. 10 [55, 56]:

$$EEXI_{\,ref.} = \left(\frac{A}{B^{\,C}}\right)\left(1 - \frac{X}{100}\right) \tag{10}$$

where, A and C are the factors depending on ship type and are equal to 2253.7 and 0.474, respectively for LNG carriers. B is the vessel deadweight (DWT) in tons. X is the decrease percentage and equals 30% for LNG carriers.

The ($EEXI_{attained}$) can be represented in units of (gCO_2/ton-NM) as demonstrated in Eq. 11 [55]:

$$\begin{aligned} EEXI_{attained} &= \frac{\left[\prod_{j=1}^{M} f_j \left(\sum_{i=1}^{nME} P_{ME(i)} \cdot SFC_{ME(i)} \cdot C_{FME(i)}\right)\right] + \left[SFC_{AE} \cdot C_{FAE} \cdot P_{AE}\right]}{Transport\ work} \\ &+ \frac{\left[\left(\prod_{j=1}^{n} f_j \cdot \sum_{i=1}^{nPTI} P_{PTI(i)} - \sum_{n=1}^{n_{eff}} f_{eff(i)} \cdot P_{AEeff(i)}\right) C_{FAE} \cdot SFC_{AE}\right] - \left[\sum_{i=1}^{n_{eff}} f_{eff(i)} \cdot P_{eff(i)} \cdot C_{FME} \cdot SFC_{ME}\right]}{Transport\ work} \end{aligned} \tag{11}$$

where, the parameter $P_{ME(i)}$ represents the power output of the vessel's main engines, while P_{AE} denotes the power output of the auxiliary engines. SFC_{AE} signifies the fuel consumption per gram hour of the diesel generator, and $SFC_{ME(i)}$ represents the fuel consumption per gram hour of the prime mover. The variables CF_{AE} and $CF_{ME(i)}$ represent the fuel conversion factors of the auxiliary and main engines to CO_2. $P_{PTI(i)}$ corresponds to the power taken in by the shaft generator. Additionally, $P_{AEff(i)}$ and $P_{eff(i)}$ represent the power saved by utilizing advanced technology systems, taking into account their availability factors $f_{eff(i)}$. The equations for calculating P_{AE}, transport work, and other variables mentioned in Eq. 10 can be found in references [55-57]. Finally, the determination of the boil-off gas rate from LNG carriers can be accomplished by referring to previous studies such as [58-60].

In addition, the operational carbon intensity indicator (*CII*) is employed for the assessment of ship CO_2 emissions. Similar to the *EEXI*, the attained *CII* value should be lower than or equal to the reference *CII* standard established by IMO. The reference *CII* value (gCO_2/ton-NM) for LNG carriers can be calculated using Eq. 12 [61]:

$$CII_{\,reference} = 9.827 \times DWT\left(1 - \frac{Re}{100}\right) \tag{12}$$

where Re is the percentage of reduction in the reference *CII* value variance depending on the operational year. These reduction percentages range from 1% to 11% for the years from 2020 to 2026 [62].

On the other hand, the attained *CII* value (gCO_2/ton-NM) can be calculated using Eq. 13 [62, 63]:

$$CII_{attained} = \frac{\sum_i \sum_j FC_{ij} \cdot C_{F(j)}}{\sum_i DWT \cdot D_i} \tag{13}$$

where the variables *i* and *j* represent the trip number and the fuel type, respectively. *FC* represents the fuel consumption in tons, while C_F denotes the fuel conversion variable for CO_2 emissions. *D* represents the distance traveled in nautical miles.

2.2 Economic Modelling

The economic element represents the backbone of any development in the maritime field, where ship economics plays the main role in adopting the application of modern technology and is the most influential factor in determining the extent to which it can be applied, alongside the technical dimensions. A simple economic model can be formulated through which the economic impact resulting from the use of any of the previously explained technical proposals can be evaluated.

For the combined DE and FR propulsion system (DE-FR), the total cost (C_{T1}) is presented by the cost of DE engines (C_{DE}) and the cost of FR (C_{FR}), as shown in Eq. 14a:

$$C_{T1} = C_{DE} + C_{FR} \tag{14a}$$

The cost of DE engines, C_{DE}, includes the capital, operating, and other additional costs as described in Eq. 14b:

$$C_{DE} = \sum_{k=1}^{m} [\{P_{DE} \,.\, S_T \,.SFC_k \,.\, F_k \,.[1 \pm p\_i].10^{-6}\} + P_{DE} \,.\, C_{DE} \,.\{1 + ins_{DE}\}\ ] \tag{14b}$$

where P_{DE} is the available diesel engine power rating, S_T is the sailing time, SFC_k is the specific fuel consumption, F_k denotes diesel fuel price, p_i is the fuel price increment/reduction percent, C_{DE} is the unit power cost, and ins_{DE} is the installing cost of the diesel engines.

Additionally, the cost of FR, C_{FR}, can be formulated as shown in Eq. 14c:

$$C_{FR} = [N_{FR}.P_{FR} \,.\, C_C \,.(1 + I_C)] + \left[N_{FR} \,.\, S_T \,.\left\{\left[P_c \,.\, SFC_{GE} \,.\, F_{C_{GE}}(1 \pm p_i) \,.10^{-6}\right] + \sum_{a=1}^{n} C_{S_a}\right\}\right] + \sum_{b=1}^{m} C_{V_b} \tag{14c}$$

where N_{FR} is the number of rotors, P_{FR} is the net power of one rotor, C_C is the capital cost of one rotor in \$/kW, I_C is the installation cost in percent, $C_{O\&S_a}$ is the operating and service costs in dollars, C_{V_b} represents any additional costs related to this system in dollars, such as insurance, classification societies, and weight effect. Moreover, the operating and service costs are directly affected by the consumed power needed for the rotor motor, supplied from the electric generators (P_c) in kW, the electric generator specific fuel consumption (SFC_{GE}) in g/kWh, the electric generator fuel price ($F_{C_{GE}}$) in dollars per ton, the rotor specific maintenance cost (C_{S_a}) in dollars per operating hour, and the ship sailing time (S_T) in hours.

In the case of the combined DFE and FR propulsion system (DFE-FR), the total cost (C_{T2}) can be calculated using Eq. 15:

$$C_{T2} = C_{DF} + C_{FR} \tag{15}$$

where C_{DF} presents the cost of the DF engine, which can be calculated using Eq. 15a:

$$C_{DF} = \left\{ P_{DF} . \ C_{DF} \ . \ (1 + ins_{DF}) \ + \sum_{x=1}^{2} \left[P_{DF\ x} . S_T * \ SFC_x \ . \ F_x (1 \pm p_i) . 10^{-6} \right] + \sum_{y=1}^{L} S_T * C_{M_{DF}} \right\} \tag{15a}$$

where P_{DF} is the output power of DFE in kilowatts, C_{DF} is the capital cost of DFE in \$/kW, ins_{DF} is the percentage of installation cost compared with the capital cost, SFC is the specific fuel consumption, F is the fuel price, p is the change in fuel price, x represents the fuel type (either diesel oil or natural gas), and C_{MDF} is the maintenance cost of DFE engines in dollars.

In the case of a combined COGAS and FR propulsion system (COGAS-FR), the total cost (C_{T3}) can be calculated using Eq. 16:

$$C_{T3} = C_{COGAS} + C_{FR} \tag{16}$$

where C_{COGAS} presents the total costs of the COGAS engines which can be estimated using Eq. 16a:

$$C_{COGAS} = \left\{ \left[P_{CO} . \ C_{CO} \ . \ (1 + ins_{CO}) + \sum C_{CO} \right] + \left[\sum_{z=1}^{2} \left[S_{T_z} . P_{CO\ z} . \ SFC_z \ . \ F_z (1 \pm p_i) \ . 10^{-6} \right] \right] \right\} \tag{16a}$$

where P_{CO} is the output power of the gas turbine in kW, C_{CO} is the cost of the power unit in \$/kW, ins_{CO} represents the installation cost fraction, $C_{M_{CO}}$ is the maintenance cost, SFC_z is the specific fuel consumption of the COGAS system, F_z is the fuel cost, and z represents the fuel type.

To determine the annual cost of a specific propulsion engine, the formula expressed in Eq. 17 will be used, considering an interest rate of (i) over a specific number of working years (N) [64, 65]:

$$C_A = \left\{ C_T \ . \ \frac{i \ [1 + i \ ]^N}{[1 + i]^N - 1} \right\} \tag{17}$$

As all energy projects aim to reduce the cost of energy production, the value of the localized cost of energy ($LCOE$) is estimated to compare between the two proposed systems, with reference to the specific unit of energy, as shown in Eq.18. $LCOE$ is a measure of the average net present cost of electricity produced from a specific energy source over its lifetime [18, 66, 67]:

$$LCOE = \frac{\sum_{t=1}^{x} \frac{C_I + C_O + C_M}{[1+r\ ]^t}}{\frac{E_t}{[1+r]^t}} \tag{18}$$

where, C_I, C_O, and C_M represent the investment expenditures, operating expenditures, and maintenance expenditures, respectively, in dollars of a certain propulsion system in the year (t). Additionally, E_t represents the total produced energy by this system in kWh over the same lifetime, taking into account the discount rate (r).

2.3 Model validation

In general, the validation of mathematical models is essential for ensuring their accuracy, reliability, and credibility, which are fundamental for making informed decisions, advancing scientific understanding, and solving real-world problems effectively. The validation of the present FR model is based on previous studies' data. Both the model used in this study as well as the models compared in the literature share an aspect ratio of 6. In Fig. 3, a comparison is presented between the rotor power consumption in kW and the lift force in kN for the chosen Norsepower model [13], which has an elevation of 24 m and a radius of 2 m. Fig. 2a displays

the comparison of rotor power consumption between the current study and that of [44, 68]. It is crucial to note that the low values of the power coefficient in [68], especially for spin ratios exceeding 1.5, can be attributed to the omission of friction losses. On the other hand, Fig. 2b confirms the results for the lift force, showing that the lift coefficient values in the present study fall within the range of the verified models. Therefore, the comparison of rotor power consumption and lift force demonstrates good agreement across various spin ratios up to 3.0.

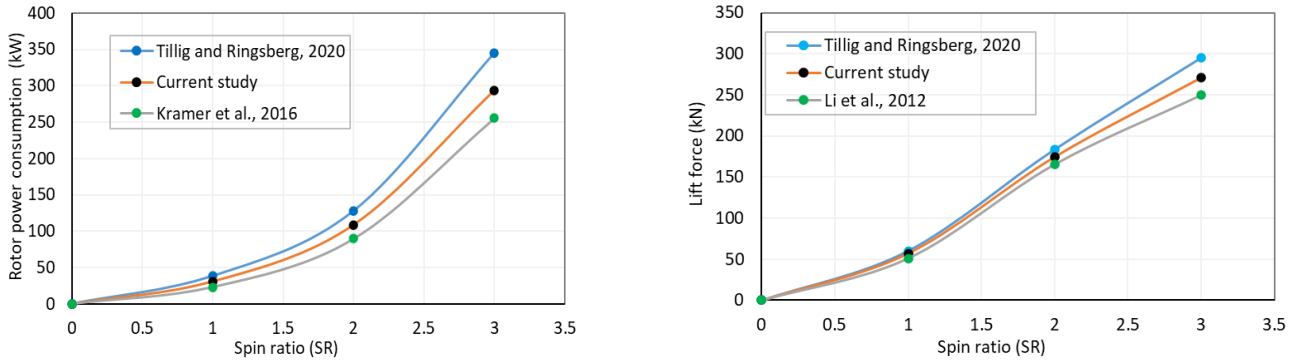

(a) Rotor power consumption (b) Lift force

Fig. 3 Validation for the FR model

3. LNG carrier case study and assumptions

WILFORCE (IMO: 9627954) is an LNG Tanker that was built in 2013 (10 years ago) and has been sailing under the flag of Malta. Her carrying capacity is 155,900 cubic meters of liquid gas, and her current draught is reported to be 9.7 meters. She has an overall length (LOA) of 290 meters and a width of 44.04 meters. The main vessel's particulars are presented in Table 1 [69-71]. The total installed propulsion and auxiliary powers for the ship are 34,200 kW and 10,500 kW, respectively. The propulsion system features one dual-fuel main engine connected to a fixed-pitch propeller, while the auxiliary generator sets are capable of burning natural gas.

Table 1 Main particulars of the WILFORCE LNG Carrier

IMO number	9627954
Ship's Main Dimensions (L, B, d)	280.96 m / 44.04 m / 12.52 m
Displacement/ Deadweight	120487.4 ton / 87749.6 ton
Gross tonnage	102315 ton
Total cubic capacity 98%	152886.94 m³
Tank capacities (ballast)	56821.8 m³
Service speed	17 knots
Propulsion power	34,200 kW
Auxiliary engines	3x3,500 kW

WILFORCE, an LNG Tanker, operates in the Mediterranean Sea along a fixed route from the LNG terminal at Damietta Port in Egypt to the LNG terminal of Cartagena Port in Spain. Fig. 4a depicts the ship's route, starting from Damietta and passing through the territorial waters of Egypt, Malta, Tunisia, and Algeria before reaching the Cartagena LNG terminal in Spain. On the other hand, Fig. 4b showcases the suggested locations of six FRs on the vessel's main deck. The rotors will be strategically spread throughout the ship's length to ensure they do not obstruct the movement of the crew.

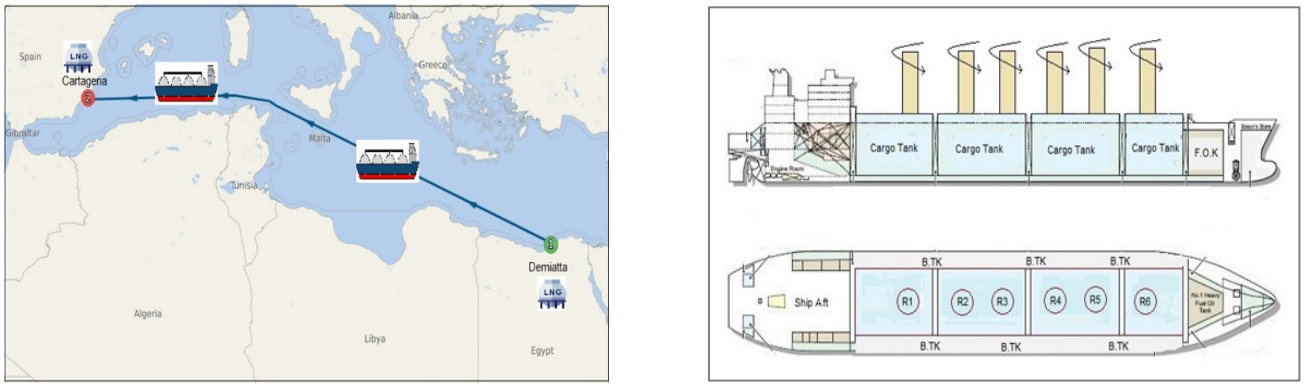

(a) Vessel route (b) Flettner rotor's locations

Fig. 4 Vessel's route and Flettner rotor's locations onboard the case study

The representative vessel operational profile for the WILFORCE LNG Carrier is characterized in Fig. 5 [69-71]. These processes may exhibit slight variations across different voyages. It is worth noting that the vessel cruises from Damietta to Fos Cavaou port and returns to Damietta port in approximately 12 to 13 days, depending on the wind and water current in the sailing area. The vessel's speed fluctuates around 17 knots. Furthermore, the vessel stays at anchorage areas and ports for cargo handling for approximately 4 to 5 days, depending on the instructions from LNG terminals, to complete a two-way trip in an approximately 12-day span.

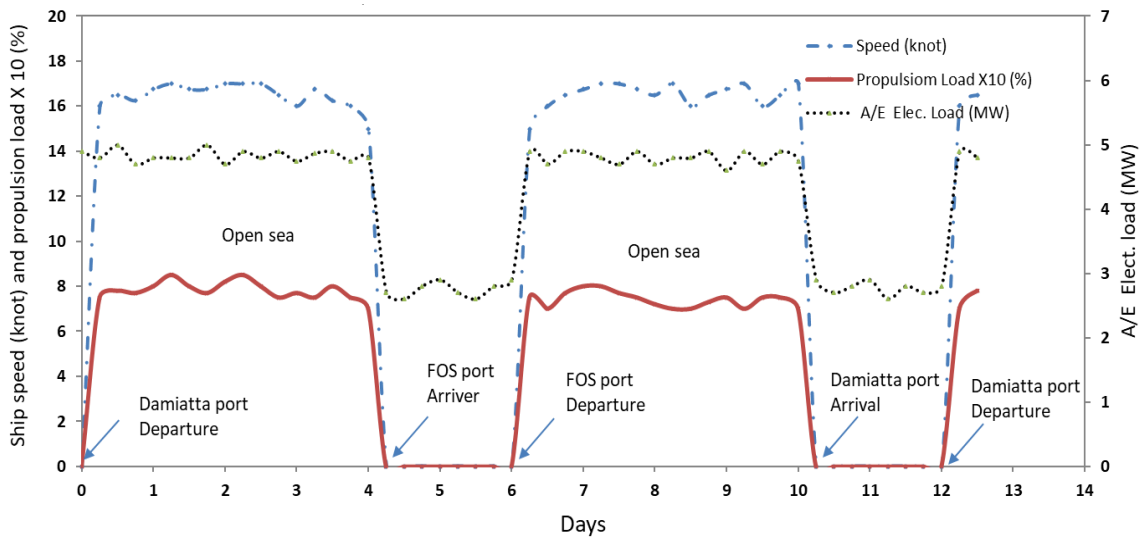

Fig. 5 Operational profile for the WILFORCE LNG Carrier.

The assumptions made in this study are as follows: The vessel follows a consistent route at a steady pace, transporting from Damietta port in Egypt to Fos Cavaou port in France. The chosen FR model is the Norsepower FR [13, 72], with dimensions of 24m in height and 4m in diameter, weighing approximately 34 tons. The electric motor powering the rotor operates at a flexible speed of up to 225 rpm. This model is effective within different wind velocities, generating an effective thrust of up to 175 kN. The installation of the FR does not significantly impact vessel stability and displacement. However, under headwind conditions, where the resultant forces produced by the rotors oppose the vessel's direction of motion, all the rotors are supposed to be non-operational. The technical calculations for the FR are conducted using a vessel speed of 17 knots during open sea cruising, taking into account different true wind angles. Factors such as vessel drift angle and bearing resistance are ignored. The vessel propulsion system efficiency is supposed to be 56% [44, 48, 73, 74], and the wind characteristics and direction data are obtained from meteoblue weather statistics [75].

The net output power of FR is assessed by considering true wind characteristics, speeds and directions, and ship routes. To determine the weights for true wind speeds, the wind speed data is analyzed using a probability density function (*pdf*) represented by Eq. 19 [76]. Wind characteristic data is used to develop a weighing scheme for true wind speeds, as illustrated in Table 2. It is evident from the table that the true wind speed of 5 m/s has a high probability distribution through the different seasons of the year. Therefore, the current study assumes constraints on the true wind speed based on the ship's route to be 5 m/s. Additionally, a spin ratio of 1.5 is assumed for this study.

$$W = \frac{\int_{x_1}^{x_2} pdf\ dx}{\int_{0}^{x_{max}} pdf\ dx} \tag{19}$$

Table 2 Weights assigned to true wind speeds at various seasons for the vessel route

Wind speed range (m/s)	0-4.17	4.17-8.33	8.33-12.5	>12.5
Wind speed (m/s)	2.22	5	8.61	14.72
Mid-season	0.102	0.402	0.114	0.001
Summer	0.007	0.289	0.008	0.0001
Winter	0.168	0.483	0.198	0.003

With respect to the economic feasibility, the main cost items and the necessary assumptions are related to the unit power cost, which is assumed to be \$420, \$530, \$960, and \$5200 per kilowatt (kW) for DE, DFE, COGAS, and FR, respectively [77, 78]. The installation cost is assumed to be 10% of the total capital cost. The fuel price is taken as the average of the last three months, which is \$550, \$700, and \$420 for heavy fuel, diesel fuel, and LNG fuel, respectively, with expectations of a 5% increment in the coming years [79].

4. Results and discussions

In this section, the results obtained from installing six FRs on the case study vessel are investigated for three different propulsion engines: the DE, DFE, and COGAS. The DE propulsion system is assumed to operate on heavy fuel oil (HFO) and low sulfur fuel (LSF). The DE(HFO) system is assumed to incorporate a selective catalytic reduction system (SCR) and a seawater scrubber (SWS) system to reduce NO_x and SO_x emissions, respectively, while the DE(LSF) uses only an SCR system. On the other hand, the DFE system operates on a combination of 5% MDO and 95% natural gas (NG), while the COGAS system utilizes NG fuel.

The findings are presented in two sections. The initial section focuses on the primary techno-environmental outcomes of the FR model. Primary parameters considered in the technical analysis consist of true wind characteristics and the spin ratio specific to the installed FR model. The environmental benefits, specifically the EEXI and CII, are evaluated for the case study. Additionally, the financial implications and the levelized cost of energy associated with the utilization of FR on the WILFORCE ship are also investigated.

4.1 Technical and environmental results

The polar plot in Fig. 6 (left side) depicts the relationship between the net output powers of a single FR in kilowatts (kW) at varying true wind and vessel speeds from 5 knots to 17 knots. This plot specifically calculates the output power at a ship speed of 17 knots across wind directions spanning the full 360°. In contrast, Fig. 6 (right side) calculates the output power under typical wind conditions of 5.0 m/s along the chosen ship route across different wind angles. The Figure demonstrates a gradual increase in net output power as both ship and true wind speeds increase. Consequently, implementing slow steaming will lead to longer voyage durations and reduced net output power generated by Flettner rotors. Based on the chosen FR model, the maximum net output powers are 279 kW, 483 kW, and 749 kW at true wind speeds of 5 m/s, 8 m/s, and 11 m/s, respectively, with a constant true wind angle of 105 degrees and a vessel speed of 17 knots. Ultimately,

the average net output power for each FR, considering the chosen case study, vessel route, and rotor model, amounts to 209 kW, resulting in a total power of 1254 kW for six Flettner rotors.

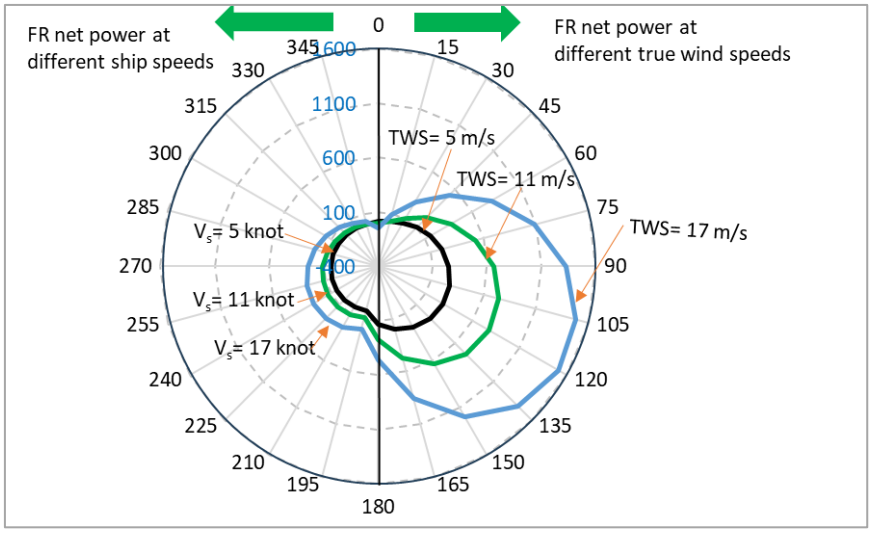

Fig. 6 Rotor sail net output power at various true wind and vessel speeds

In addition, the spin ratio (SR) is a significant factor influencing the net output power of rotor sails, as it determines the lift coefficient and the thrust generated. Consequently, it affects the FR power in relation to the ship's heading. Fig. 7a illustrates the net output power of one FR at various spin ratios, ranging from 0.5 to 2.5, based on the selected FR model. This model was chosen considering the available upper deck area in the current case study. The results were executed at an average vessel speed of 17 knots and an average true wind speed of 5 m/s. As the spin ratio increases, the power output also increases. This is a result of the increased thrust force in the ship's direction. On the other hand, Fig. 7b compares the fuel consumption of the three investigated propulsion engines: DE, DFE, and COGAS. The diesel fuel consumption for the DE propulsion system is reduced by 963.1 tons per year with a reduction percentage of 3.67% after the installation of six Flettner rotors onboard. Similarly, the fuel savings for the DFE and COGAS propulsion engines are 1251 tons per year and 1222 tons per year, respectively, with reduction percentages of 3.67% and 2.86%.

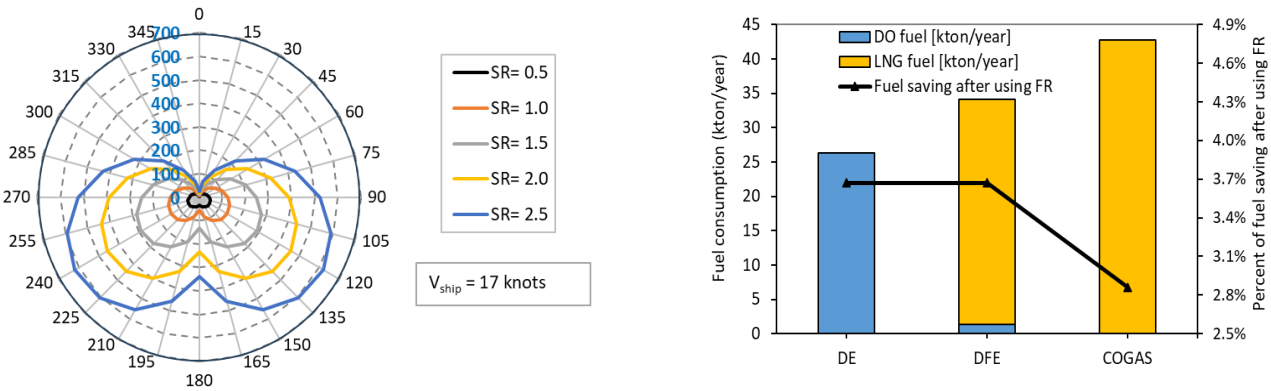

(a) Effect of spin ratio (b) Fuel consumption and saving

Fig. 7 Effect of spin ratio on FR output power as well as fuel consumption and saving

By utilizing equations 8 and 9 in addition to the data on fuel consumption reduction resulting from the installation of FR onboard the case study, as revealed in Fig. 7b, it is possible to calculate the corresponding emission reduction values. Fig. 8 presents the reduction values in SO_x, NO_x, CO_2, HC, and CO emissions across a variety of true wind orientations spanning from 0 to 360 degrees, specifically for the diesel engine propulsion system operated by low sulfur fuel. These values are calculated based on the characteristics data for the ship route, as well as the average true wind speed of 5 m/s and vessel speed of 17 knots. Among these emissions, the highest reduction values are observed in CO_2 emissions. At a true wind angle of 120 degrees and 240 degrees, the maximum reductions in NO_x, SO_x, and CO_2 emissions are 11.84 Mg/year, 13.56 Mg/year,

and 44.11 Gg/year, respectively. These reductions can be attributed to the significant aerodynamic lift and effective power generated by the FR at these orientations.

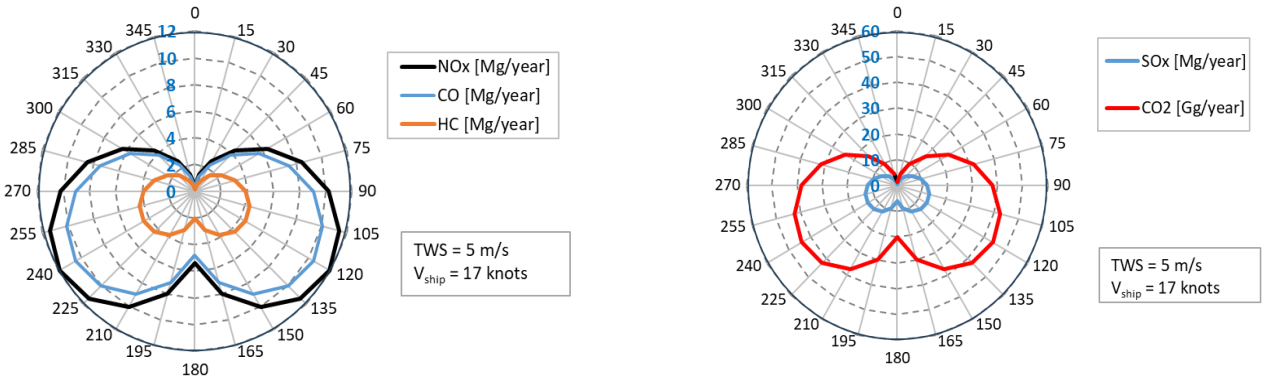

(a) NO_x, CO, and HC emissions (b) SO_x and CO_2 emissions

Fig. 8 Ship emission reduction after installing FR at different true wind angles

Furthermore, ship emissions can be calculated using the ship fuel consumption method. This approach involves estimating emissions based on the quantity and type of fuel consumed by the vessel. Emission factors specific to the fuel type, expressed in grams per kilowatt-hour (g/kWh), are utilized to approximate emissions of pollutants such as CO_2, SO_x, NO_x, and particulate matter. Fig. 9 provides a comparison of the three investigated propulsion systems, namely DE-FR, DFE-FR, and COGAS-FR, with six Flettner rotors installed onboard. It evaluates their relative NO_x emissions to IMO Tier III standards in both cruise and maneuvering modes, as well as their relative SO_x emissions to IMO 2020 limits. Importantly, it should be noted that all of these systems conform to the IMO standards for SO_x and NO_x emissions. By incorporating FR into the DE (HFO), DE (LSF), DFE, and COGAS systems on the case study ship, reductions of 9.15, 8.56, 16.72, and 4.82 tons per year, respectively, can be achieved in NO_x emissions. Additionally, the COGAS system exhibits no SO_x emissions, while the DE (HFO), DE (LSF), and DFE systems can achieve reductions of 55.78, 9.81, and 0.98 tons per year, respectively. These findings highlight the significant potential of FR in reducing both NO_x and SO_x emissions, thereby contributing to enhanced environmental sustainability in maritime operations.

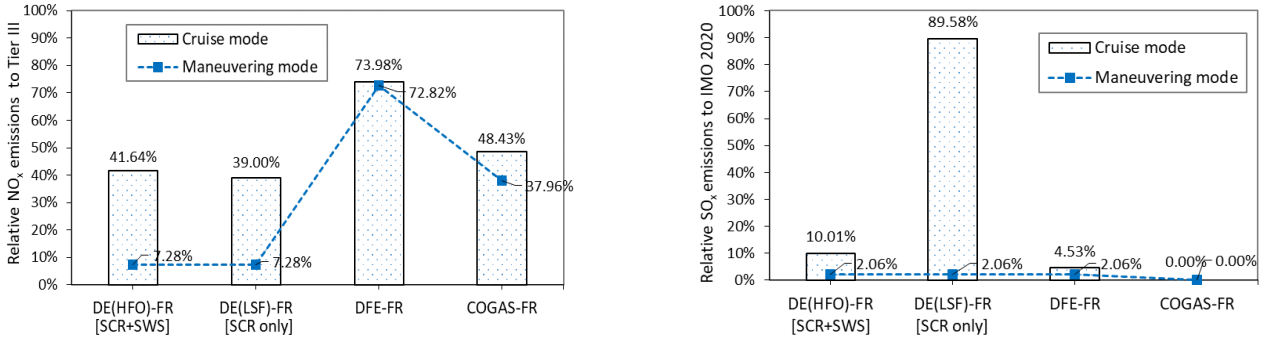

(a) NO_x emissions comparison (b) SO_x emissions comparison

Fig. 9 Effect of FRon NO_x and SO_x emissions compared with IMO regulations

Moreover, Fig. 10 illustrates the correlation between the three examined propulsion engines, namely DE, DFE, and COGAS, both with and without FR, and their Energy Efficiency Existing Ship Index (EEXI) at varying ship speeds. The reference EEXI value for the target vessel, with a Deadweight Tonnage (DWT) of 87,750 tons, is established at 7.16 gCO_2/ton.nm. Notably, the installation of FR on the ship leads to significant enhancements in the EEXI value, with a 3.6% improvement for DE and DFE propulsion systems and a 4.68% enhancement for the COGAS propulsion system. It is observed that as ship speed increases, the attained EEXI value decreases with the maximum design ship speed set at 22 knots. To meet the reference EEXI value, the minimum ship speeds required for the COGAS-FR, DFE-FR, and DE-FR systems are

determined as 17.5, 19.8, and 21.1 knots, respectively. These results underscore the positive impact of integrating FR on ship energy efficiency, leading to improved EEXI values, and emphasize the importance of considering ship speed to meet regulatory EEXI requirements.

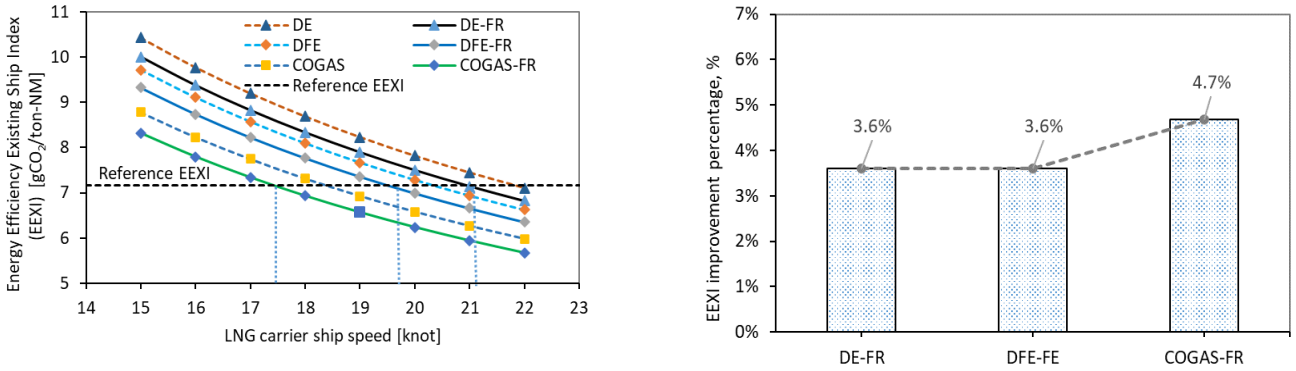

(a) EEXI at various ship speeds (b) EEXI improvement percentages

Fig. 10 EEXI at various ship speeds and improvement after installing Flettner rotors

Additionally, Fig. 11 illustrates the relationship between the reference CII values for the years 2020 to 2026 and the calculated CII values for the case study, specifically focusing on the DFE-FR and COGAS-FR propulsion engines at ship speeds ranging from 13 to 22 knots. The Figure includes five rating categories (labeled A to E) recommended by the IMO. CII values falling within ratings D and E indicate poorer performance, as they slightly deviate from the reference CII values set for the upcoming years. Conversely, CII values below the reference CII are preferred, particularly those falling within ratings A to C, indicating better performance. For the DFE-FR system, ship speeds ranging from 16 to 22 knots are preferred to comply with the reference CII 2024 values established by the IMO, corresponding to ratings A to C. Ship speeds of 13 and 14 knots yield worse ratings, falling into the unpreferred categories of E and D, respectively. On the other hand, for the COGAS-FR system, a wide range of ship speeds starting from 14 knots is preferred, with no speeds falling within the D and E categories. Ultimately, the minimum ship speeds that achieve the highest carbon intensity rating scores, aligning with the IMO recommendations until 2026, are 15 knots for COGAS and 17 knots for DFE. These findings highlight the importance of selecting appropriate ship speeds to attain desired CII ratings and comply with IMO requirements, ultimately contributing to improved carbon intensity performance in maritime operations.

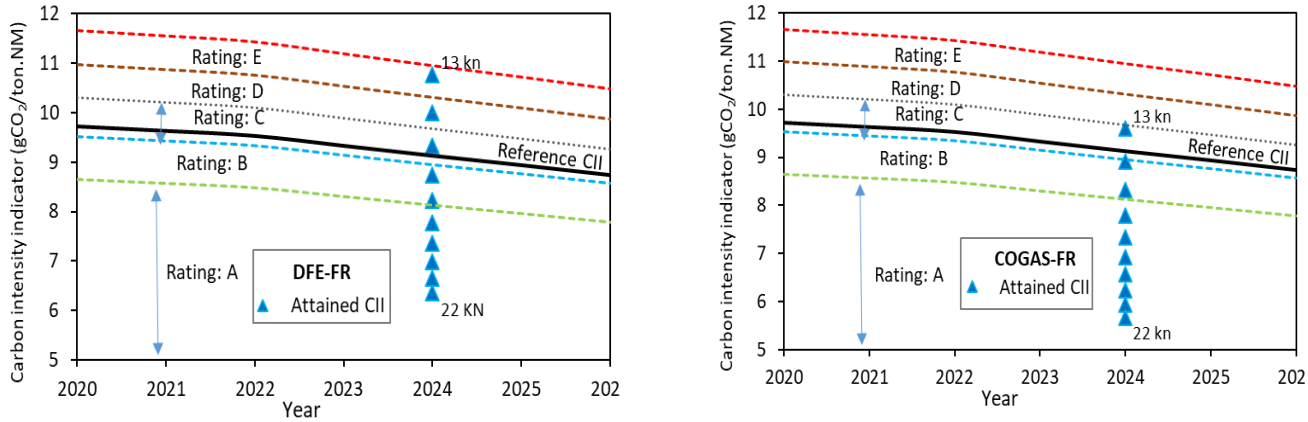

(a) DFE-FR propulsion system (b) COGAS-FR propulsion system

Fig. 11 Effect of FR on carbon intensity indicator (CII) at various ship speeds

Finally, the technical and environmental results have revealed that the implementation of FR on ships has several positive effects. Increasing ship and true wind speeds have resulted in a gradual increase in net output power, while slow steaming has decreased power output. Higher spin ratios have also been found to increase power output. The installation of FR has led to reductions in fuel consumption and significant

reductions in CO_2 emissions, with some reductions observed in NO_x emissions as well. The study has also found that FR has improved the EEXI values, with the DE, DFE, and COGAS propulsion systems showing improvements of 3.6% and 4.68%. Higher ship speeds have been associated with lower EEXI values, and specific ship speeds have been required to meet the reference EEXI value for each system. Regarding the CII values, the minimum ship speeds that achieve the highest carbon intensity rating scores, aligning with the IMO recommendations until 2026, are 15 knots for COGAS and 17 knots for DFE.

4.2 Economic results

The current economic analysis investigates the influence of employing FR as an auxiliary propulsion system and compares various proposed propulsion systems for the case study from diverse economic perspectives. Referring to the Flettner rotors, Fig. 12a indicates the possibility of installing the FR at the lowest annual capital cost of $510,000 per year if they are not replaced over the ship's lifetime. Additionally, the Figure demonstrates the change in operating cost and total cost of the Flettner rotors, amounting to $150 million and $155 million, respectively, at the end of the ship's lifetime. The total cost exhibits a decline until approximately the seventh year before gradually increasing.

Fig. 12b displays the economic benefit resulting from using FR as part of the total ship's propulsion power compared to achieving the same power from other systems. The Figure illustrates that the FRs are not economically viable before the tenth year of the ship's lifetime. However, after this period, the FR became an economic solution, resulting in savings in ship operating costs by $40.9 million, $37.4 million, and $34.1 million compared to the DE, DFE, and COGAS propulsion systems, respectively, by the end of the ship's lifetime.

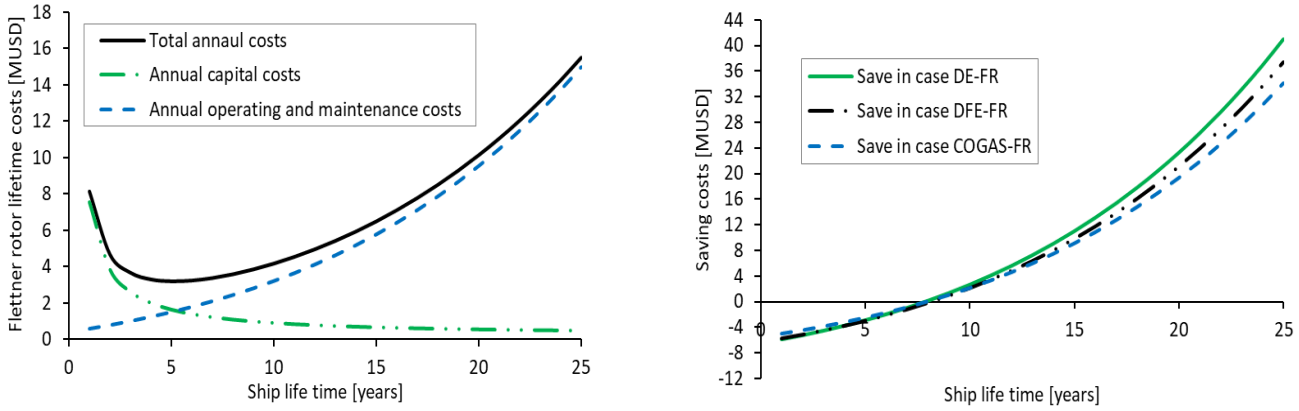

(a) FR total annual costs (b) FR saving costs

Fig. 12 FR economic aspects over the ship's lifetime

In the same context, the economic results of the proposed propulsion systems reveal several influential facts, of which, the most important is the type of fuel and its price. These findings support the significance of the study, which primarily aims to shift towards alternative fuels.

Fig. 13a displays the expected annual capital cost of each system over the ship's lifetime. It is notable that the COGAS-FR system initially exhibits a significantly higher capital cost compared to the other two systems, surpassing them by more than two times. Additionally, the capital cost of DFE-FR is close to that of DE-FR. However, as the expected ship lifespan increases, the differences among the three systems become less pronounced, with differences of $1.62 million, $1.97 million, and $3.96 million for the DE-FR, DFE-FR, and COGAS-FR systems, respectively.

In contrast, Fig. 13b illustrates the operating and maintenance costs for the proposed propulsion systems. It is evident that the COGAS-FR system has the highest costs, followed by the DE-FR system, while the DFE-FR system presents the lowest operating and maintenance costs. Moreover, the Figure indicates a continuous increment in costs among the three systems over the ship's working years, resulting in a difference of approximately $300 million between the highest and lowest costs by the end of the ship's expected lifetime.

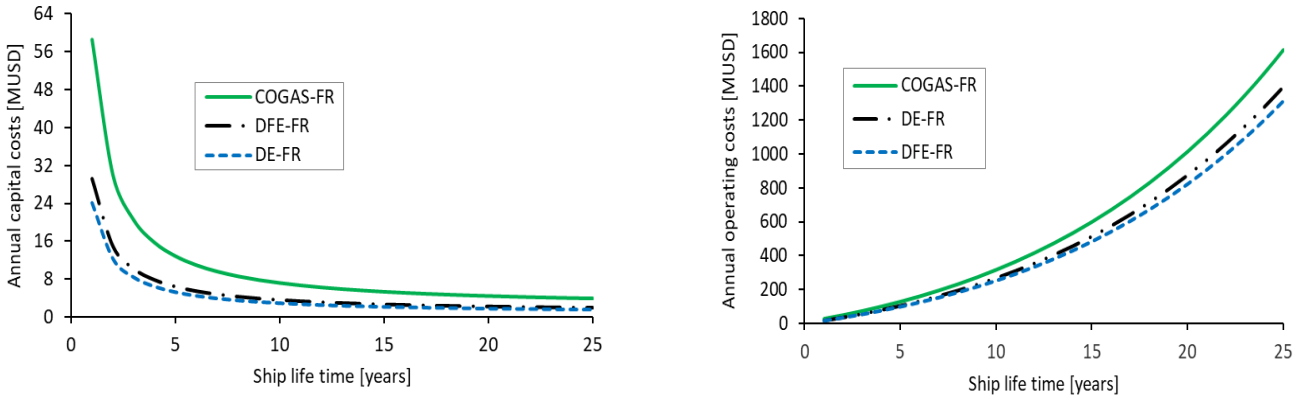

(a) Capital costs for different systems (b) Operating costs for different systems

Fig. 13 Annual Capital and operating costs of the different engines integrated with FR

Fig. 14 illustrates the cost savings that can be achieved or required when using each of the proposed systems compared to the DE-FR system operating with heavy fuel oil and diesel oil. From the Figure, it is evident that neither the DF-FR nor the COGAS-FR system will be economically viable over the ship's lifetime when compared to the DE-FR system fueled by heavy oil. On the other hand, when compared to the DE system operating with diesel oil, the DF-FR system will start yielding economic benefits after five years of the ship's lifespan. Furthermore, the Figure demonstrates the potential for achieving cost savings of $78.1 million by the end of the ship's working years if the DFE-FR system is utilized. However, the COGAS-FR system remains uneconomical and would result in a substantial loss of ship profit.

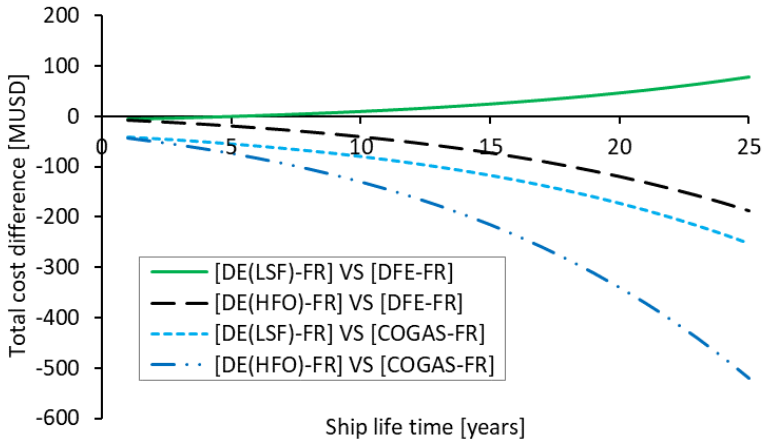

Fig. 14 Ship saving cost vs. ship working years in different scenarios

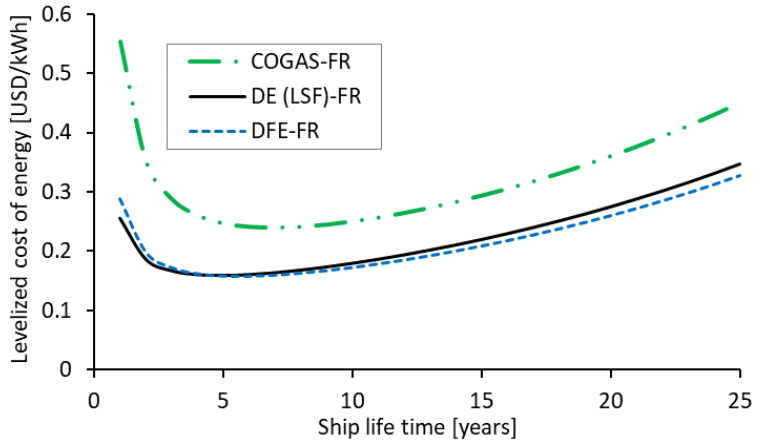

Fig. 15 LCOE for the different propulsion systems at the ship's lifetime

Fig. 15 demonstrates the levelized cost of energy for the different systems, at a discount rate of 5%. It is evident that this value decreases as the ship's lifetime increases, starting from 0.25, 0.29, and 0.55 $/kWh and reaching the lowest values of 0.16, 0.16, and 0.24 $/kWh for the DE-FR, DFE-FR, and COGAS-FR systems, respectively, at a working time of 5 years. However, it begins to increase to 0.35, 0.32, and 0.45 $/kWh for the DE-FR, DFE-FR, and COGAS-FR systems, respectively, at the end of the ship's lifetime.

To evaluate the environmental benefits of measures aimed at reducing exhaust gas emissions and considering their annual costs, an assessment of the annual cost-effectiveness is conducted. Fig. 16 showcases the cost-effectiveness plan for the DFE-FR and COGAS-FR propulsion systems in comparison to the base systems DE(HFO)-FR and DE(LSF)-FR. The DFE-FR system achieves a total lifetime emission reduction of 239.1 kton, while the COGAS-FR system achieves a reduction of 141.6 kton. When compared to the DE(HFO)-FR system, the cost-effectiveness of the DFE-FR system is calculated at $789.3/ton, whereas the COGAS-FR system has a cost-effectiveness of $3668.7/ton. In comparison to the DE(LSF)-FR system, the DFE-FR system achieves reductions of 120.5 kton, with a cost-effectiveness of $647.6/ton, and the COGAS-FR system achieves reductions of 23.1 kton, with a cost-effectiveness of $10954.6/ton. As depicted in the Figure, the DFE-FR system demonstrates greater cost-effectiveness at a lower cost when compared to the DE(LSF)-FR system. However, the COGAS-FR system proves to be effective in reducing emissions, albeit at a higher cost.

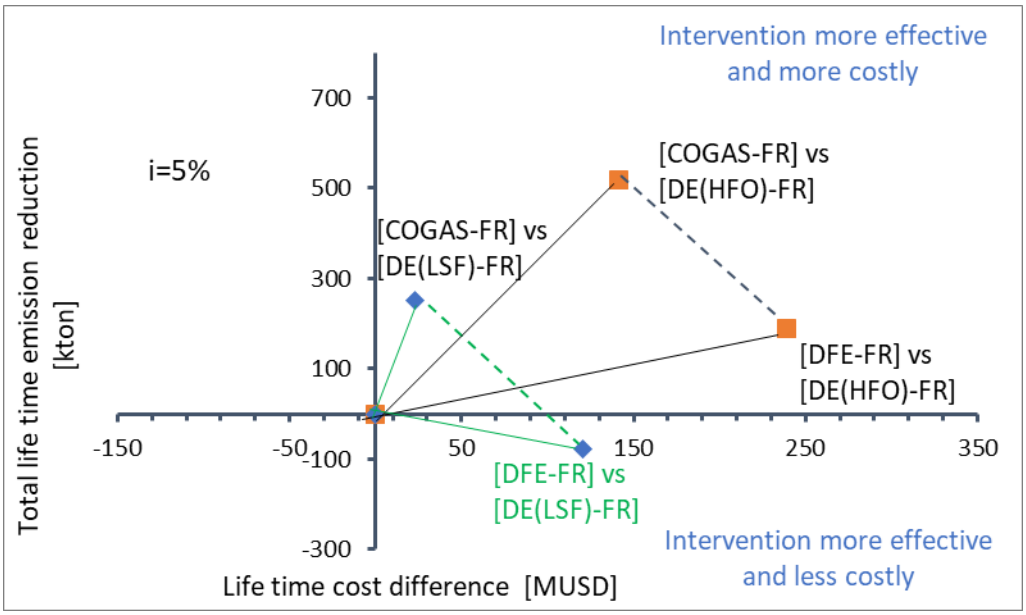

Fig. 16 Cost-effectiveness plane for the investigated systems integrated with Flettner rotors

The above economic results highlight several key findings when comparing the propulsion system that utilizes DFE-FR or COGAS-FR and the system that uses DE. The most crucial among these findings is the significance of the fuel type employed in marine propulsion systems. The results indicate that when compared with DE (HFO), the economic feasibility diminishes. However, in the case of DE (LSF), an economic benefit can be achieved. Notably, as the expected working years of the ship increase, the DFE-FR system emerges as the most favorable economic option. Furthermore, the results demonstrate that an economic benefit can be attained by considering the cost of energy production per unit on the ship. The LCOE shows a reduction of approximately 9.85% in the case of DFE-FR compared with the conventional system.

Finally, in the context of the assumptions presented in the paper, several factors are expected to exert a substantial influence on operating conditions and results in real exploitation scenarios. The assumption of a consistent wind speed of 5 m/s along the ship's route is likely to have a notable impact, as real-world wind speeds can vary significantly, affecting the efficiency and performance of the FR system. Moreover, the effectiveness of the chosen Norsepower FR model across different wind velocities and its ability to generate thrust up to 175 kN are critical assumptions that may vary in practice based on changing wind speeds. The assumption that the installation of the FR does not significantly impact vessel stability and displacement could

be crucial, given that such additions can indeed affect the vessel's dynamics. Additionally, the assumption that all rotors are non-operational under headwind conditions could significantly influence the efficiency and operation of the FR system in real-world conditions. Furthermore, the assumed propulsion system efficiency of 56% may have a notable impact on overall energy consumption and vessel performance, with real-world efficiencies likely to fluctuate based on operational conditions. In real exploitation conditions, changes in these adopted assumptions, such as the variability of wind speeds, the performance of the FR model across different wind velocities, the impact on vessel stability, and the actual propulsion system efficiency, can significantly affect the operational conditions and results when utilizing the FR system in practical maritime operations.

5. Conclusions

The current paper studies three propulsion engines for LNG carriers integrated with FR systems. These integrated systems are diesel engines (DE-FR), dual fuel engines (DFE-FR), and combined gas and steam turbine engines (COGAS-FR). The analysis is performed from technical, environmental, and economic perspectives.

From a technical viewpoint, increasing ship and true wind speeds will lead to a gradual increase in the output power of FR. Higher spin ratios also increase power output due to increased thrust force. The average net output power for one FR, considering the chosen case study, vessel route, and FR model, will be 209 kW/hr, resulting in a total power of 1254 kW for six Flettner rotors. The maximum reductions in emissions occur when facing wind directions of 120 degrees and 240 degrees for the selected rotor model. The implementation of six FRs will lead to fuel consumption reductions, with the DE, DFE, and COGAS propulsion engines achieving reductions of 963.1 tons per year (3.67%), 1251 tons per year (3.67%), and 1222 tons per year (2.86%), respectively.

From an environmental viewpoint, the COGAS-FR system emerges as the most favorable option, reducing NO_x emissions by 4.82 tons per year and having no SO_x emissions. On the other hand, the DFE-FR system is the second-best choice, achieving reductions of 16.72 and 0.98 tons per year in NO_x and SO_x emissions, respectively. Moreover, the COGAS-FR and DFE-FR propulsion systems will improve EEXI value by 4.68% and 3.6%, respectively. To meet the reference EEXI value, minimum ship speeds of 17.5 knots and 19.8 knots are required for the COGAS-FR and DFE-FR systems, respectively. When considering CII values, the COGAS system offers a wider range of compatible operational ship speeds, aligning with the IMO recommendations compared to the DFE system. The minimum ship speeds that achieve the highest carbon intensity rating scores, aligning with the IMO recommendations until 2026, are 15 knots for COGAS and 17 knots for DFE.

From an economic perspective, the research presents an economic comparison among the proposed propulsion systems. Neither the DFE-FR nor the COGAS-FR system will be an economical option when compared to the DE(HFO)-FR system. However, the DFE-FR system will achieve an economic benefit when compared to the DE(LSF), resulting in cost savings of $78.1 million. Conversely, the COGAS-FR system will remain a non-economic choice. The lowest values of LCOE (Levelized Cost of Energy) for the different systems are 0.16, 0.16, and 0.24 $/kWh for the DE-FR, DFE-FR, and COGAS-FR systems, respectively. These values increase to reach 0.35, 0.32, and 0.45 $/kWh, over the ship's lifetime. Moreover, the DFE-FR system demonstrates greater cost-effectiveness at a lower cost when compared with the DE(LSF)-FR system. However, the COGAS-FR system proves to be effective in reducing emissions at a higher cost.

Finally, future studies stemming from the research paper's findings could delve into the long-term performance and durability of the different propulsion configurations identified, assessing their reliability and maintenance requirements over extended periods of operation. Additionally, investigating the scalability of integrating NG fuel with FR technology across diverse vessel types and sizes within the maritime industry could provide insights into the widespread applicability of these sustainable solutions. Addressing the limitations of the current study, future research could focus on conducting field trials or pilot projects to validate the model predictions in real-world conditions, enhancing the robustness and practical relevance of the findings. Moreover, global contributions of this research could involve comparative analyses with similar

studies in different regions to understand the contextual factors influencing the adoption of alternative propulsion systems and to highlight best practices for promoting sustainable practices in the international maritime sector. By exploring these future research avenues, bridging existing gaps, and building upon the study's outcomes, the maritime industry can further progress toward achieving its sustainability goals and reducing environmental impact.

Nomenclature

Ar	Effective rotor area, m^2
ARE	Annual reduction in emissions, ton/year
ASF	Annual fuel saving, ton/year
C_A	Annual cost, $
C_{COGAS}	Cost of COGAS engines, $
C_D	Drag coefficient
C_{DF}	Cost of dual fuel engines, $
C_F	Fuel conversion factor to CO_2 emissions
C_{FR}	Costs of Flettner rotors, $
C_L	Lift Coefficient
C_T	Total costs, $
CII	Carbon intensity indicator, gCO_2/ton-NM
D	Drag force, N
DWT	Ship deadweight, ton
EEDI	Energy efficiency design index, gCO_2/ton-NM
E_F	Engine emission factor, kg/kWh
i	Annual interest rate, %
L	Lift force, N
LOCE	localized cost of energy, $/kWh
N	Ship working years
P_{prod}	Flettner rotor produced power, kW
P_{cons}	Flettner rotor consumed power, kW
Pi	Fuel price increment/reduction percent, %
SFC	Specific fuel consumption, g/kWh
V_{aw}	Apparent wind speed, m/s
V_{tw}	True wind speed, m/s
V_s	Ship's speed, knots

Abbreviations

CO_2	carbon dioxide
COGAS	Combined gas and steam
DE	Diesel engine
DFE	Dual fuel diesel engine
FR	Flettner rotor
HFO	Heavy fuel oil
IMO	International Maritime Organization
LNG	Liquefied natural gas
LSF	Low sulfur fuel
NO_x	Nitrogen oxides
SO_x	Sulfur oxides

REFERENCES

[1] UNFCC.,2022. Sharm el-Sheikh Climate Change Conference - climate action. https://unfccc.int/cop27. accessed 20th December 2023.

[2] IMO., 2020. Fourth IMO GHG study 2020. Full Report. International Maritime Organization, London. https://www.imo.org/en/OurWork/Environment/Pages/Fourth-IMO-Greenhouse-Gas-Study-2020.aspx. accessed 10th February 2024.

[3] IMO., 2018. Marine Environment Protection Committee (MEPC), 72nd session. https://www.imo.org/en/MediaCentre/MeetingSummaries/Pages/MEPC-72nd-session.aspx. accessed 10th December 2023.

[4] IMO, Reduction of GHG emissions from ships. Fourth IMO GHG Study 2020 – Final report. MEPC 75/7/15. 2020.

[5] IMO., 2019. Sulphur oxides (SOx) and Particulate Matter (PM) – Regulation 14. https://www.imo.org/en/OurWork/Environment/Pages/Sulphur-oxides-(SOx)-%E2%80%93-Regulation-14.aspx. accessed 22nd December 2023.

[6] IMO., 2019. Nitrogen Oxides (NOx) – Regulation 13. https://www.imo.org/en/OurWork/Environment/Pages/Nitrogen-oxides-(NOx)-%E2%80%93-Regulation-13.aspx. accessed 22nd December 2023.

[7] IMO., 2020. EEXI and CII - ship carbon intensity and rating system. https://www.imo.org/en/MediaCentre/HotTopics/Pages/EEXI-CII-FAQ.aspx. accessed 1st February 2024.

[8] IMO, Guidance on treatment of innovative energy efficiency technologies for calculation and verification of the attained EEDI and EEXI, MEPC.1/Circ.896. 2021.

[9] Elkafas, A.G., M. Rivarolo, A.F. Massardo, 2023. Environmental economic analysis of speed reduction measure onboard container ships. *Environmental Science and Pollution Research*, 30(21), 59645-59659. https://doi.org/10.1007/s11356-023-26745-4

[10] Mahía Prados, J. M., Arias Fernández, I., Romero Gómez, M., Naveiro Parga, M., 2024. The decarbonisation of the maritime sector: Horizon 2050. *Brodogradnja*, 75(2), 1-26. https://doi.org/10.21278/brod75202

[11] Nuttall, P., Newell, A., Prasad, B., Veitayaki, J., Holland, E., 2014. A review of sustainable sea-transport for Oceania: Providing context for renewable energy shipping for the Pacific. *Marine Policy*, 43, 283-287. https://doi.org/10.1016/j.marpol.2013.06.009

[12] Harahap, F., Nurdiawati, A., Conti, D., Leduc, S., Urban, F., 2023. Renewable marine fuel production for decarbonised maritime shipping: Pathways, policy measures and transition dynamics. *Journal of Cleaner Production*, 415, 137906. https://doi.org/10.1016/j.jclepro.2023.137906

[13] Norsepower. 2023. Norsepower Rotor Sail Saving fuel and the planet, For bulkers, tankers, RoRos, ferries, LNG carriers, RoPaxes, and passenger ships. https://www.norsepower.com/app/uploads/2023/08/brochure_ENG_screen.pdf. accessed 21st December 2023.

[14] Thies, F. Fakiolas, K., 2022. Chapter 8 - Wind propulsion. *Sustainable Energy Systems on Ships, Novel Technologies for Low Carbon Shipping*, 353-402. https://doi.org/10.1016/B978-0-12-824471-5.00016-5

[15] Zhang, P., Lozano, J., Wang, Y., 2021. Using Flettner Rotors and Parafoil as alternative propulsion systems for bulk carriers. *Journal of Cleaner Production*, 317, 128418. https://doi.org/10.1016/j.jclepro.2021.128418

[16] Alkhaledi, A., Sampath, S., Pilidis, P., 2023. Techno environmental assessment of Flettner rotor as assistance propulsion system for LH_2 tanker ship fuelled by hydrogen. *Sustainable energy technologies and assessments*, 55, 102935. https://doi.org/10.1016/j.seta.2022.102935

[17] Ammar, N.R. Seddiek, I.S., 2022. Wind assisted propulsion system onboard ships: case study Flettner rotors. *Ships and Offshore Structures*, 17(7), 1616-1627. https://doi.org/10.1080/17445302.2021.1937797

[18] Seddiek, I.S. Ammar, N.R., 2021. Harnessing wind energy on merchant ships: case study Flettner rotors onboard bulk carriers. *Environmental Science and Pollution Research*, 28(25), 32695-32707. https://doi.org/10.1007/s11356-021-12791-3

[19] Karslen, R., Papachristos, G., Rehmatulla, N., 2019. An agent-based model of climate-energy policies to promote wind propulsion technology in shipping. *Environmental innovation and societal transitions*, 31, 33-53. https://doi.org/10.1016/j.eist.2019.01.006

[20] Lu, R.H., Ringsberg, J.W., 2020. Ship energy performance study of three wind-assisted ship propulsion technologies including a parametric study of the Flettner rotor technology. *Ships and offshore structures*, 15(3), 249-258. https://doi.org/10.1080/17445302.2019.1612544

[21] Bordogna, G., Muggiasca, S., Giappino, S., Belloli, M., Keuning, J.A., Huijsmans, R.H.M., van 't Veer, A.P., 2019. Experiments on a Flettner rotor at critical and supercritical Reynolds numbers. *Journal of wind engineering and industrial aerodynamics*, 188, 19-29. https://doi.org/10.1016/j.jweia.2019.02.006

[22] Bordogna, G., Muggiasca, S., Giappino, S., Belloli, M., Keuning, J.A., Huijsmans, R.H.M., 2019. The effects of the aerodynamic interaction on the performance of two Flettner rotors. *Journal of wind engineering and industrial aerodynamics*, 196(3), 104024. https://doi.org/10.1016/j.jweia.2019.104024

[23] Li, B., Zhang, R., Zhang, B., Yang, Q., Guo, C., 2021. An assisted propulsion device of vessel utilizing wind energy based on Magnus effect. *Applied Ocean Research*, 114, 102788. https://doi.org/10.1016/j.apor.2021.102788

[24] Kume, K., Hamada, T., Kobayashi, H., Yamanaka, S., 2022. Evaluation of aerodynamic characteristics of a ship with Flettner rotors by wind tunnel tests and RANS-based CFD. *Ocean Engineering*, 254, 111345. https://doi.org/10.1016/j.oceaneng.2022.111345

[25] Chen, W.L., Wang, H.F., Liu, X.Y., 2023. Experimental investigation of the aerodynamic performance of Flettner rotors for marine applications. *Ocean Engineering*, 281, 115006. https://doi.org/10.1016/j.oceaneng.2023.115006

[26] Zhang, R., Huang, L., Wang, K., Ma, R., Ruan, Z., Wang, C., 2024. Novel optimized layout for Flettner rotors based on reuse of wake energy. *Journal of Cleaner Production*, 443, 140922. https://doi.org/10.1016/j.jclepro.2024.140922

[27] Kwon, C.S., Yeon, S.M., Kim, Y.C., Kim, Y.G., Kim, Y. H., Kang, H. J., 2022. A parametric study for a Flettner rotor in standalone condition using CFD. *International Journal of Naval Architecture and Ocean Engineering*, 14, 100493. https://doi.org/10.1016/j.ijnaoe.2022.100493

[28] Copuroglu, H.I. Pesman, E., 2018. Analysis of Flettner Rotor ships in beam waves. *Ocean Engineering*, 150, 352-362. https://doi.org/10.1016/j.oceaneng.2018.01.004

[29] Mason, J., Larkin, A., Gallego-Schmid, A., 2023. Mitigating stochastic uncertainty from weather routing for ships with wind propulsion. *Ocean Engineering*, 281, 114674. https://doi.org/10.1016/j.oceaneng.2023.114674

[30] Sauder, T., Alterskjær, S.A., 2022. Hydrodynamic testing of wind-assisted cargo ships using a cyber–physical method. *Ocean Engineering*, 243, 110206. https://doi.org/10.1016/j.oceaneng.2021.110206

[31] Arabnejad, M.H., Thies, F., Yao, H-D., Ringsberg, J.W., 2024. Zero-emission propulsion system featuring, Flettner rotors, batteries and fuel cells, for a merchant ship. *Ocean Engineering*, 310, 118618. https://doi.org/10.1016/j.oceaneng.2024.118618

[32] Livaniou, S., Papadopoulos, G.A., 2022. Liquefied Natural Gas (LNG) as a transitional choice replacing marine conventional fuels (heavy fuel oil/marine diesel oil), towards the era of decarbonisation. *Sustainability*, 14(24), 16364. https://doi.org/10.3390/su142416364

[33] Elgohary, M.M., Seddiek, I.S., and Salem, A.M., 2015. Overview of alternative fuels with emphasis on the potential of liquefied natural gas as future marine fuel. *Proceedings of the Institution of Mechanical Engineers, Part M: Journal of Engineering for the Maritime Environment*, 229(4), 365-375. https://doi.org/10.1177/1475090214522778

[34] Tuswan, T., Sari, D. P., Muttaqie, T., Prabowo, A. R., Soetardjo, M., Murwantono, T. T. P., Utina, R., Yuniati, Y., 2023. Representative application of LNG-fuelled ships: a critical overview on potential GHG emission reductions and economic benefits. *Brodogradnja*, 74(1), 63-83. https://doi.org/10.21278/brod74104

[35] Lu, Z., Ma, M., Wang, T., Lu, T., Wang, H., Feng, Y., Shi, L., 2023. Numerical research of the in-cylinder natural gas stratification in a natural gas-diesel dual-fuel marine engine. *Fuel*, 337, 126861. https://doi.org/10.1016/j.fuel.2022.126861

[36] Yu, H., Wang, W., Sheng, D., Li, H., Duan, S., 2022. Performance of combustion process on marine low speed two-stroke dual fuel engine at different fuel conditions: Full diesel/diesel ignited natural gas. *Fuel*, 310, 122370. https://doi.org/10.1016/j.fuel.2021.122370

[37] Pham, V.C.; Choi, J.-H.; Rho, B.-S.; Kim, J.-S.; Park, K.; Park, S.-K.; Le, V.V.; Lee, W.-J. A., 2021. Numerical study on the combustion process and emission characteristics of a natural gas-diesel dual-fuel marine engine at full load. *Energies*, 14(5), 1342. https://doi.org/10.3390/en14051342

[38] Gan, H., Wang, H., Tang, Y., Wang, G., 2020. Investigation of the miller cycle on the performance and emission in a natural gas-diesel dual-fuel marine engine by using two zone combustion model. *Thermal Science*, 24(1), 259-270. https://doi.org/10.2298/TSCI190518420G

[39] Alzayedi, A.M.T., Batra, A., Sampath, S., Pilidis, P., 2022. Techno-environmental mission evaluation of combined cycle gas turbines for large container ship propulsion. *Energies*, 15(12), 4426. https://doi.org/10.3390/en15124426

[40] Dotto, A., Campora, U., Satta, F., 2021. Feasibility study of an integrated COGES-DF engine power plant in LNG propulsion for a cruise-ferry. *Energy conversion and management*, 245, 114602. https://doi.org/10.1016/j.enconman.2021.114602

[41] Barsi, D., Costa, C., Satta, F., Zunino, P., Busi, A., Ghio, R., Raffaeli, C., Sabattini, A., 2020. Design of a mini combined heat and power cycle for naval applications. *Journal of Sustainable Development of Energy, Water and Environment Systems*, 8(2), 281-292. https://doi.org/10.13044/j.sdewes.d7.0309

[42] Welaya, Y.M.A., Mosleh, M., Ammar, N.R., 2014. Thermodynamic analysis of a combined solid oxide fuel cell with a steam turbine power plant for marine applications. *Brodogradnja*, 65(1), 97-116.

[43] Naveiro, M., Gómez, M. R., Arias-Fernández, I., Baaliña Insua, Á., 2023. Energy, exergy, economic and environmental analysis of a regasification system integrating simple ORC and LNG open power cycle in floating storage regasification units. *Brodogradnja*, 74(2), 39-75. https://doi.org/10.21278/brod74203

[44] Tillig, F., Ringsberg, J.W., 2020. Design, operation and analysis of wind-assisted cargo ships. *Ocean Engineering*, 211, 107603. https://doi.org/10.1016/j.oceaneng.2020.107603

[45] Vigna, V., Figari M., 2023. Wind-Assisted ship propulsion: matching Flettner rotors with diesel engines and controllable pitch propellers. *Journal of Marine Science and Engineering*, 11(5), 1072. https://doi.org/10.3390/jmse11051072

[46] Traut, M., Gilbert, P., Walsh, C., Bows, A., Filippone, A., Stansby, P., Wood, R., 2014. Propulsive power contribution of a kite and a Flettner rotor on selected shipping routes. *Applied Energy*, 113, 362-372. https://doi.org/10.1016/j.apenergy.2013.07.026

[47] Li, D., Leer-Andersen, M., Allenstrom, B., 2012. Performance and vortex formation of Flettner rotors at high Reynolds numbers. *29th International Symposium on Naval Hydrodynamics*, 26-31 August, Gothenburg, Sweden.

[48] Lele, A., Rao, K.V.S., 2017. Net power generated by Flettner rotor for different values of wind speed and ship speed. *International Conference on Circuit, Power and Computing Technologies (ICCPCT)*, Kollam, India. https://doi.org/10.1109/ICCPCT.2017.8074170

[49] Ammar, N.R., Seddiek, I.S., 2020. An environmental and economic analysis of emission reduction strategies for container ships with emphasis on the improved energy efficiency indexes. *Environmental Science and Pollution Research*, 27, 23342–23355. https://doi.org/10.1007/s11356-020-08861-7

[50] Ammar, N.R., Seddiek, I.S., 2017. Eco-environmental analysis of ship emission control methods: Case study RO-RO cargo vessel. *Ocean Engineering*, 137,166-173. https://doi.org/10.1016/j.oceaneng.2017.03.052

[51] IMO, 2018. Report of the Working Group on Reduction of greenhouse gas emissions from ships. MEPC 72/WP.7. London.

[52] IMO, 2019. Draft report of the Marine Environmental Protection Committee on its seventy-fourth session. MEPC74/WP.1. London.

[53] Trozzi, C., De Lauretis, R., 2023. Air pollutant emission inventory guidebook. Technical report, European Environmental Agency. http: www// eea.europa.eu. accessed 15th February 2024.

[54] Fernández, I. A., Gómez, M. R., Gómez, J. R., Insua, Á. B., 2017. Review of propulsion systems on LNG carriers. *Renewable and Sustainable Energy Reviews*, 67, 1395-1411. https://doi.org/10.1016/j.rser.2016.09.095

[55] IMO. 2021. Guidelines on the method of calculation of the attained Energy Efficiency Existing Ship Index (EEXI). Resolution MEPC.333(76). https://wwwcdn.imo.org/localresources/en/KnowledgeCentre/IndexofIMOResolutions/MEPCDocuments/MEPC.333(76).pdf. accessed 5h March 2024.

[56] ABS. 2022. Energy Efficiency Existing Ship Index (EEXI). https://ww2.eagle.org/content/dam/eagle/regulatory-news/2022/ABS%20Regulatory%20News%20-%20EEXI.pdf. accessed 16h December 2023.

[57] IACS. 2022. EEXI Implementation Guidelines. https://iacs.org.uk/download/14308. accessed 10th December 2023.

[58] IMO. 2018. Report of the marine environment protection committee on its sixty-second session. http://www.crs.hr/Portals/0/MEPC%2062-24.pdf. accessed 21st December 2023.

[59] Ahn, J., You, H., Ryu, J., Chang, D., 2017. Strategy for selecting an optimal propulsion system of a liquefied hydrogen tanker. *International Journal of Hydrogen Energy*, 42(8), 5366-5380. https://doi.org/10.1016/j.ijhydene.2017.01.037

[60] Ammar, N.R., 2019. Environmental and cost-effectiveness comparison of dual fuel propulsion options for emissions reduction onboard LNG carriers. *Brodogradnja*, 70(3), 61-77. https://doi.org/10.21278/brod70304

[61] IMO. 2022. Resolution MEPC.353(78): Guidelines on the reference lines for use with operational carbon intensity indicators. https://wwwcdn.imo.org/localresources/en/OurWork/Environment/Documents/Air%20pollution/MEPC.353(78).pdf. accessed 8th May 2023.

[62] IMO. 2021. Resolution MEPC.352(78): Guidelines on operational carbon intensity indicators and the calculation methods. https://wwwcdn.imo.org/localresources/en/OurWork/Environment/Documents/Air%20pollution/MEPC.339(76).pdf. accessed 9th May 2023.

[63] IMO. 2021. Guidelines on the operational carbon intensity reduction factors relative to reference lines.: https://www.mardep.gov.hk/en/msnote/pdf/msin2302anx13.pdf. accessed 8th May 2023.

[64] Hwang, I., Park, C., Jeong, B., 2023. Life cycle cost analysis for Scotland short-sea ferries. *Journal of Marine Science and Engineering*, 11(2), 424. https://doi.org/10.3390/jmse11020424

[65] Seddiek, I.S., Ammar, N.R., 2023. Technical and eco-environmental analysis of blue/green ammonia-fueled RO/RO ships. *Transportation Research Part D: Transport and Environment*, 114, 103547. https://doi.org/10.1016/j.trd.2022.103547

[66] Barelli, L., Bidini, G., Cinti, G.,2020. Operation of a solid oxide fuel cell based power system with ammonia as a fuel: experimental test and system design. *Energies*, 13(23), 6173. https://doi.org/10.3390/en13236173

[67] Liang, Y., Ma, Y., Wang, H., Mesbahi, A., Jeong, B., Zhou, P., 2021. Levelized cost of energy analysis for offshore wind farms – A case study of the New York State development. *Ocean Engineering*, 239, 109923. https://doi.org/10.1016/j.oceaneng.2021.109923

[68] Kramer, J., Steen, S., Savio, L.,2016. Drift forces – wing sails vs Flettner rotors, *International Conference on High Performance Marine Vehicles*, 17-19 October, Cortona, Italy.

[69] Vessel Finder. 2023. WILFORCE LNG Tanker, IMO 9627954. https://www.vesselfinder.com/vessels/details/9627954. accessed 2nd December 2023.

[70] Baltic Shipping. 2024. WILFORCE, IMO 9627954. https://www.balticshipping.com/vessel/imo/9627954. accessed 2nd February 2024.

[71] Fleet moon. 2023. WILFORCE. https://www.fleetmon.com/vessels/wilforce_9627954_8472619/. accessed 22nd December 2023.

[72] Norsepower. 2023. Norsepower rotor sail solution. http://wind-ship.org/wp-content/uploads/2018/08/Norsepower-Rotor-Sail-Solution-brochure-2018.pdf. accessed 10th February 2024.

[73] MAN. *Basic principles of ship propulsion*. https://www.man-es.com/docs/default-source/document-sync/basic-principles-of-ship-propulsion-eng.pdf. accessed 20th September 2024.

[74] Anthony, F.M., Turnock, S.R., Hudson, D.A. 2017. Ship resistance and propulsion: Practical Estimation of Ship propulsive power. Cambridge University Press. https://doi.org/10.1017/9781316494196

[75] Meteoblue, 2023. Wind speed and characteristics. https://www.meteoblue.com/en/weather/historyclimate/climatemodelled. accessed 10th December 2023.

[76] Seta, K., Wang, W., Ikegaya, N., 2023. Modeling probability density functions of instantaneous velocity components at the pedestrian levels of a building array by Gram–Charlier series. *Journal of Wind Engineering and Industrial Aerodynamics*, 239, 105427. https://doi.org/10.1016/j.jweia.2023.105427

[77] Jeong, J., Seo, S., You, H., Chang, D., 2018. Comparative analysis of a hybrid propulsion using LNG-LH_2 complying with regulations on emissions. *International Journal of Hydrogen Energy*, 43(7), 3809-3821. https://doi.org/10.1016/j.ijhydene.2018.01.041

[78] Wang, Y., Wright, L.A., 2021. A Comparative Review of Alternative Fuels for the Maritime Sector: Economic, Technology, and Policy Challenges for Clean Energy Implementation. *World*, 2, 456-481 https://doi.org/10.3390/world2040029

[79] Ship & Bunker. 2023. World Bunker Prices. https://shipandbunker.com/prices. accessed 10th December 2023.